Physics Letters B 707 (2012) 546–552

Contents lists available at SciVerse ScienceDirect

Physics Letters B

www.elsevier.com/locate/physletb

Generalized form factors and spin structures of the kaon

Seung-il Nam [a,b], Hyun-Chul Kim [c,a,*]

[a] School of Physics, Korea Institute for Advanced Study, Seoul 130-722, Republic of Korea
[b] Research Institute for Basic Sciences, Korea Aerospace University, Goyang 412-791, Republic of Korea
[c] Department of Physics, Inha University, Incheon 402-751, Republic of Korea

ARTICLE INFO

Article history:
Received 17 April 2011
Received in revised form 22 December 2011
Accepted 8 January 2012
Available online 10 January 2012
Editor: J.-P. Blaizot

Keywords:
Kaon generalized form factors
Spin structure of the kaon
Nonlocal chiral quark model from the instanton vacuum
Explicit flavor SU(3) symmetry breaking

ABSTRACT

We investigate the spin structure of the kaon, based on the nonlocal chiral quark model from the instanton vacuum. We first revisit the electromagnetic form factors of the pion and kaon, improving the results for the kaon. We evaluate the generalized tensor form factors of the kaon in order to determine the probability density of transversely polarized quarks inside the kaon. We consider the effects of flavor SU(3) symmetry breaking, so that the probability density of the up and strange quarks are examined in detail. It is found that the strange quark behaves differently inside the kaon in comparison with the up quark.

1. Recently, the QCDSF/UKQCD Collaborations reported the first lattice results for the pion transversity [1]. They evaluated the probability density of the polarized quarks inside the pion and found that their distribution in the impact-parameter space is strongly distorted when the quarks are transversely polarized. These lattice results have triggered various theoretical works [2–5]. Broniowski et al. [4] have investigated the tensor form factors of the pion within the local and nonlocal chiral quark models [4] and have employed a larger value of the pion mass, i.e. $m_\pi = 600$ MeV in such a way that the results can be compared with the lattice data directly. They also considered the case of the chiral limit. In Ref. [5], the tensor form factors of the pion were calculated and the probability density of the polarized quarks inside the pion was derived by combining the tensor form factors with the electromagnetic (EM) ones, based on the nonlocal chiral quark model (NχQM) from the instanton vacuum. The results were in good agreement with the lattice data [1].

It is also of great interest to study the spin structure of the kaon, since it sheds light on the effects of flavor SU(3) symmetry breaking on behavior of the strange quark. Thus, in the present Letter, we aim at investigating the generalized tensor form factors of the kaon and their implications for its spin structure within the framework of the NχQM [6,7]. In Ref. [7], Musakhanov extended the work of Ref. [6], considering the finite current-quark mass. Since we need to take into account the explicit breaking of flavor SU(3) symmetry breaking, we will use the extended NχQM from the instanton vacuum [7–9]. The model provides a suitable framework to study properties of the kaon, since the instanton vacuum explains the spontaneous chiral symmetry breaking (SχSB) naturally via quark zero modes and the explicit breaking of flavor SU(3) symmetry can be treated consistently. Moreover, an important merit of this approach lies in the fact that there are only two parameters, i.e. the average (anti)instanton size $\bar{\rho} \approx 1/3$ fm and average inter-instanton distance $\bar{R} \approx 1$ fm. In particular, the average size of instantons, of which the inverse is approximately equal to $\bar{\rho}^{-1} \approx 600$ MeV, provides the natural scale of the model. Note that the values of the $\bar{\rho}$ and $\bar{R}$ were estimated many years ago phenomenologically in Ref. [11] as well as theoretically in Refs. [12–14]. The present framework has been already used to describe successfully semileptonic decays of the kaon [15] and qualitatively its EM form factor [10].

In order to evaluate the probability density of the polarized quarks inside the kaon, it is essential to know quantitatively the EM form factor of the kaon. Thus, in the present work, we will take as a free parameter the constituent-quark mass at the zero virtuality of the quark rather than strictly following the previous model derived from the instanton vacuum. We will show that while properties of the pion are very stable, those of the kaon are much improved, compared to the results of the previous work [10]. We will also calculate the tensor form factors of the kaon with the two different values of the constituent-quark mass. Then, the

* Corresponding author at: Department of Physics, Inha University, Incheon 402-751, Republic of Korea.
E-mail addresses: sinam@kias.re.kr (S.-i. Nam), hchkim@inha.ac.kr (H.-C. Kim).

0370-2693
doi:10.1016/j.physletb.2012.01.016

probability density of the polarized quarks inside the kaon will be derived and discussed, based on the results of the EM and tensor form factors of the kaon. We will also study the behavior of the up and strange quarks inside the kaon, so that we understand the effects of flavor SU(3) symmetry breaking on the distribution of the strange quarks inside the kaon.

2. The generalized tensor form factors $B_{ni}(Q^2)$ of the pseudoscalar meson are defined as the matrix elements of the following tensor operator

$$\begin{aligned}&\langle\phi(p_f)|\mathcal{O}_T^{\mu\nu\mu_1\cdots\mu_{n-1}}|\phi(p_i)\rangle\\&=\mathcal{AS}\Bigg[\frac{(p^\mu q^\nu-q^\mu p^\nu)}{m_\phi}\\&\quad\times\sum_{i=\text{even}}^{n-1}q^{\mu_1}\cdots q^{\mu_i}p^{\mu_{i+1}}\cdots p^{\mu_{n-1}}B_{ni}\big(Q^2\big)\Bigg],\end{aligned}\tag{1}$$

where p_i and p_f stand for the initial and final on-shell momenta of the pseudoscalar meson ϕ, respectively. We assign the mass of the meson as m_ϕ, and also introduce respectively the average momentum and the momentum transfer $p=(p_f+p_i)/2$ and $q=p_f-p_i$. For definiteness, we will only take into account the positively charged pion (π^+) and kaon (K^+) for the meson in this work. Moreover, we set the pion and kaon masses as $m_\pi=140$ MeV and $m_K=495$ MeV as numerical input. The tensor operator can be expressed as

$$\mathcal{O}_T^{\mu\nu\mu_1\cdots\mu_{n-1}}=\mathcal{AS}\big[\bar\psi_f\sigma^{\mu\nu}\big(i\overleftrightarrow{D}^{\mu_1}\big)\cdots\big(i\overleftrightarrow{D}^{\mu_{n-1}}\big)\psi_f\big].\tag{2}$$

The operations $\mathcal{A}$ and $\mathcal{S}$ denote the anti-symmetrization in (μ,ν) and symmetrization in $(\nu,\ldots,\mu_{n-1})$ with the trace terms subtracted in all the indices. The ψ_f stands for a quark field with flavor f.

Taking into account Eqs. (1) and (2), we can define respectively the first and second generalized tensor form factors $B_{10}^{\phi,f}$ and $B_{20}^{\phi,f}$ in the momentum space as the matrix element of the tensor current, using the auxiliary-vector method as in Ref. [16]:

$$\begin{aligned}&\langle\phi(p_f)|\bar\psi_f(0)\sigma_{ab}\psi_f(0)|\phi(p_i)\rangle\\&=\big[(p_i\cdot a)(p_f\cdot b)-(p_i\cdot b)(p_f\cdot a)\big]\frac{B_{10}^{\phi,f}(Q^2)}{m_\phi},\\&\langle\phi(p_f)|\bar\psi_f(0)\sigma_{ab}(i\overleftrightarrow{D}\cdot a)\psi_f(0)|\phi(p_i)\rangle\\&=\Big\{(p\cdot a)\big[(p_i\cdot a)(p_f\cdot b)-(p_i\cdot b)(p_f\cdot a)\big]\Big\}\frac{B_{20}^{\phi,f}(Q^2)}{m_\phi},\end{aligned}\tag{3}$$

where the vectors satisfy the following conditions $a^2=a\cdot b=0$ and $b^2\neq0$, and we have used a shorthand notation $\sigma_{ab}\equiv\sigma_{\mu\nu}a^\mu b^\nu$. With the help of this auxiliary-vector method, one can eliminate the trace-term subtractions. We also use the hermitized covariant derivative $i\overleftrightarrow{D}_\mu\equiv(i\overrightarrow{D}_\mu-i\overleftarrow{D}_\mu)/2$, where D_μ indicates the SU(N_c) covariant derivative. Since we are interested in the spatial distribution of the transversely polarized quark inside the meson, we need to consider the Fourier transform of the form factors [17]:

$$\begin{aligned}\mathcal{F}^{\phi,f}\big(b_\perp^2\big)&=\frac{1}{(2\pi)^2}\int d^2q_\perp\,e^{-ib_\perp\cdot q_\perp}\mathcal{F}^{\phi,f}\big(q_\perp^2\big)\\&=\frac{1}{2\pi}\int_0^\infty Q\,dQ\;J_0(bQ)\mathcal{F}^{\phi,f}\big(Q^2\big),\end{aligned}\tag{4}$$

where $\mathcal{F}^{\phi,f}$ designates a generic flavor form factor representing, for instance, $A_{n0}^{\phi,f}$ or $B_{n0}^{\phi,f}$. The $b_\perp$ denotes the impact parameter that measures the distance from the center of momentum of the meson to the quark in the transversed plane to its motion. Here, we use $|q_\perp|\equiv Q$ and $|b_\perp|\equiv b$. The J_0 stands for the Bessel function of order zero. Similarly, the Fourier transform of the derivative of the generalized form factors with respect to $b_\perp^2$ can be evaluated as

$$\begin{aligned}\frac{\partial\mathcal{F}^{\phi,f}(b_\perp^2)}{\partial b_\perp^2}&\equiv\big[\mathcal{F}^{\phi,f}\big(b_\perp^2\big)\big]'\\&=-\frac{1}{4\pi b}\int_0^\infty Q^2\,dQ\;J_1(bQ)\mathcal{F}^{\phi,f}\big(Q^2\big).\end{aligned}\tag{5}$$

The J_1 denotes the Bessel function of order one.

The probability density of the transversely polarized quark with flavor f is defined in terms of the generalized vector and tensor form factors [1]:

$$\rho_n^{\phi,f}(b_\perp,s_\perp)=\frac{1}{2}\Bigg[A_{n0}^{\phi,f}\big(b_\perp^2\big)-\frac{s_\perp^i\epsilon^{ij}b_\perp^j}{m_\phi}\frac{\partial B_{n0}^{\phi,f}(b_\perp^2)}{\partial b_\perp^2}\Bigg],\tag{6}$$

where the $s_\perp$ stands for the fixed transverse spin of the quark. For simplicity, we choose the z direction for the quark longitudinal momentum. In the case of exact flavor SU(3) symmetry, the vector form factor $A_{10}^{\phi,f}$ with flavor f is just equal to the EM form factor due to isospin symmetry [18]: $A_{10}^{\pi,u}(Q^2)=-A_{10}^{\pi,d}(Q^2)=F_\pi(Q^2)$. Similarly, we have the following relation for the kaon: $A_{10}^{K,u}(Q^2)=-A_{10}^{K,s}(Q^2)=F_K(Q^2)$ because of V-spin symmetry. However, these simple relations are broken by explicit flavor SU(3) symmetry breaking. Hence, it is necessary to compute separately the up–down and strange form factors of the kaon.

In the previous works [5,10], the positively charged pion and kaon electromagnetic form factors were already investigated. Thus, we will employ the same theoretical framework to compute the vector form factors. Although the kaon vector form factors are different from the EM form factor of the kaon as mentioned above, they can be easily evaluated within the same framework. Therefore, we will only focus on how to evaluate the tensor form factors. For more details, one refers to Ref. [10]. Considering all the ingredients discussed so far, one is finally led to the analytical definition of the flavor probability density of the quark in the transverse impact-parameter space as follows:

$$\rho_n^{\phi,f}(b_\perp,s_x=\pm1)=\frac{1}{2}\Bigg[A_{n0}^{\phi,f}\big(b^2\big)\mp\frac{b\sin\theta_\perp}{m_\phi}\big[B_{n0}^{\phi,f}\big(b^2\big)\big]'\Bigg],\tag{7}$$

where the spin of the quark inside the meson is quantized along the x axis, $s_\perp=(\pm1,0)$.

3. We now briefly explain the extended NχQM from the instanton vacuum [7–9] and derive the generalized form factors of the pion and kaon. Considering first the dilute instanton liquid, characterized by two instanton parameters, i.e. the average (anti)instanton size $\bar\rho\approx1/3$ fm and average inter-instanton distance $\bar R\approx1$ fm with the small packing parameter $\pi\bar\rho^4/\bar R^4\approx0.1$, we are able to average the fermionic determinant over collective coordinates of instantons with fermionic quasi-particles, i.e. the constituent quarks introduced. The averaged determinant is reduced to the light-quark partition function that can be given as a functional of the tensor field in the present case. Having bosonized and integrated it over the quark fields, we obtain the following effective nonlocal chiral action in the large N_c limit in Euclidean space:

$$\mathcal{S}_{\rm eff}[m_f,\phi] = -{\rm Sp}\ln\Big[i\partial\!\!\!/ + im_f + i\sqrt{M(\partial^2)}U^{\gamma_5}(\phi)\sqrt{M(\partial^2)} + \sigma\cdot T\Big], \quad (8)$$

where m_f, ϕ, and Sp indicate the current-quark mass, the pseudo-Nambu–Goldstone (NG) boson field, and the functional trace over all relevant spaces, respectively. Assuming isospin symmetry and explicit flavor SU(3) symmetry breaking, we use the following numerical values $m_u = m_d = 5$ MeV and $m_s = 180$ MeV. The $M(i\partial)$ stands for the momentum-dependent effective quark mass, generated from the fermionic zero modes of the instantons [6]. Its analytical form is in general given by

$$M(\partial^2) = M_0 F^2(t),$$
$$F(t) = 2t\Big[I_0(t)K_1(t) - I_1(t)K_0(t) - \frac{1}{t}I_1(t)K_1(t)\Big]. \quad (9)$$

Here, $t = |\partial\!\!\!/|\bar{\rho}/2$, and I_n and K_n stand for the modified Bessel functions with the order n. In the numerical calculations, instead of using Eq. (9), we will make use of the following parametrization for numerical convenience:

$$M(\partial^2) = M_0\left(\frac{2}{2+\bar{\rho}^2\partial^2}\right)^2, \quad (10)$$

where M_0 indicates the constituent-quark mass at zero quark virtuality and its value is determined by the self-consistent equation of the instanton model in the chiral limit [7–9]:

$$\frac{1}{\bar{R}^4} = 4N_c\int\frac{d^4p}{(2\pi)^4}\frac{M^2(p)}{p^2+M^2(p)}, \quad (11)$$

resulting in $M_0 \approx 350$ MeV. As done in Refs. [7,8,19], M_0 is modified due to the explicit flavor symmetry breaking in the following way:

$$M_0 \to M_0 f(m_f) = M_0\left[\sqrt{1+\frac{m_f^2}{d^2}} - \frac{m_f}{d}\right], \quad (12)$$

where $d = 198$ MeV. We will call this model with the original set of parameters as *model I*. Note that M_0 should be modified in such a way that the instanton-number density is independent of the finite current-quark mass [7,8,19]. On the other hand, considering theoretical uncertainties in the instanton framework for the flavor SU(3) sector, we still can choose the value of M_0 to reproduce experimental data such as the pion and kaon electric-charge radii, setting $f(m_f) = 1$ in Eq. (12), from a very phenomenological point of view, whereas the instanton parameters remain unchanged. We call this phenomenological way as *model II*. The pseudo-NG boson field is represented in a nonlinear form as [20]:

$$U^{\gamma_5}(\phi) = \exp\left[\frac{i\gamma_5(\lambda\cdot\phi)}{F_\phi}\right] = 1 + \frac{i\gamma_5(\lambda\cdot\phi)}{F_\phi} - \frac{(\lambda\cdot\phi)^2}{2F_\phi^2} + \cdots, \quad (13)$$

where ϕ^α is the flavor SU(3) multiplet defined as

$$\lambda\cdot\phi = \begin{pmatrix} \frac{\pi^0}{\sqrt{2}} + \frac{\eta}{\sqrt{6}} & \pi^+ & K^+ \\ \pi^- & -\frac{\pi^0}{\sqrt{2}} + \frac{\eta}{\sqrt{6}} & K^0 \\ K^- & \bar{K}^0 & -\frac{2\eta}{\sqrt{6}} \end{pmatrix}, \quad (14)$$

where the trace over the isospin space is defined by ${\rm tr}[\lambda^\alpha\lambda^\beta] = 2\delta^{\alpha\beta}$. The F_ϕ denotes the weak-decay constant for the pseudo-NG bosons, whose empirical values are 93.2 MeV for the pion and 113 MeV for the kaon for instance. The last term in Eq. (8) denotes $\sigma\cdot T = \sigma_{\mu\nu}T_{\mu\nu}$, where $\sigma_{\mu\nu} = i[\gamma_\mu,\gamma_\nu]/2$ and $T_{\mu\nu}$ designates the external tensor field.

The three-point correlation function in Eq. (3) can be easily calculated by a functional differentiation with respect to the pseudo-NG boson and external tensor fields. Having performed the functional trace and that over color space, we can write the matrix elements for the $B_{10}^{\phi,f}(Q^2)$ and $B_{20}^{\phi,q}(Q^2)$, corresponding to Eq. (3), as follows:

$$\begin{aligned}
&\big\langle\phi(p_f)\big|q^\dagger(0)\sigma_{ab}q(0)\big|\phi(p_i)\big\rangle \\
&= -\frac{2N_c}{F_\phi^2}\int\frac{d^4k}{(2\pi)^4} \\
&\quad\times{\rm Tr}_\gamma\left[\frac{1}{i\bar{p}\!\!\!/_1}\sqrt{M_1}\gamma_5\sqrt{M_2}\frac{1}{i\bar{p}\!\!\!/_2}\sqrt{M_2}\gamma_5\sqrt{M_3}\frac{1}{i\bar{p}\!\!\!/_3}\sigma_{ab}\right], \\
&\big\langle\phi(p_f)\big|q^\dagger(0)\sigma_{ab}(i\overleftrightarrow{D}\cdot a)q(0)\big|\phi(p_i)\big\rangle \\
&= -\frac{2N_c}{F_\phi^2}\int\frac{d^4k}{(2\pi)^4} \\
&\quad\times{\rm Tr}_\gamma\left[\frac{1}{i\bar{p}\!\!\!/_1}\sqrt{M_1}\gamma_5\sqrt{M_2}\frac{1}{i\bar{p}\!\!\!/_2}\sqrt{M_2}\gamma_5\sqrt{M_3}\frac{1}{i\bar{p}\!\!\!/_3}\sigma_{ab}\eta\right], \quad (15)
\end{aligned}$$

where $\eta \equiv (k + \frac{p_i}{2})\cdot a$. The relevant momenta are also defined as

$$k_1 = k - \frac{p_i}{2} - \frac{q}{2}, \qquad k_2 = k + \frac{p_i}{2} - \frac{q}{2},$$
$$k_3 = k + \frac{p_i}{2} + \frac{q}{2}. \quad (16)$$

Here, we have used the notation $M_i \equiv M(k_i^2)$ for $i = (1,2,3)$. The denominators become $\bar{p}\!\!\!/_i = k\!\!\!/_i + i\bar{M}_i$ in Eq. (15), where $\bar{M}_i = M_i + m_i$. For $B_{n0}^{K,u}$, we choose $m_{1,3} = m_u$ and $m_2 = m_s$, while we set $m_{1,3} = m_s$ and $m_2 = m_u$ for $B_{n0}^{K,s}$. In order to evaluate the matrix element, we define the initial and final pion momenta in the Breit (brick-wall) frame in Euclidean space as done in Ref. [10]. We also have chosen the auxiliary vectors explicitly as $a = (0,1,0,i)$ and $b = (1,0,1,0)$, which satisfy the conditions mentioned previously, and have defined $\sigma_{ab} = \sigma_{\mu\nu}a^\mu b^\nu$. The momentum-dependent effective quark mass $M_{a,b,c}$ can be also defined by using Eqs. (10) and (16).

4. We now present the numerical results and discuss them. First, in order to see the reliability of the present framework, we have computed the positive-charged pion and kaon EM form factors. Moreover, the vector form factors can be easily derived from them. In the left panel of Fig. 1, we draw the numerical results for the EM form factors of the pion and kaon, using model I and model II, separately. Note that the results of model I are the same as those given in Ref. [10] as they should be. As for the pion, the results from the two models almost coincide with each other because of the small masses of the light quarks in comparison to the renormalization point $\mu \simeq 600$ MeV, and turn out to be in good agreement with the experimental data taken from Refs. [21–26]. This renormalization-point value is proportional to the inverse of the average (anti)instanton size, i.e. $\mu \approx 1/\bar{\rho}$ [11–14], indicating the scale of the quark–(anti)instanton interaction strength. Though model I provides considerably good results, we made fine-tuning of the value of M_0 to be 343 MeV for model II to fit the electric-charge radius of the pion $\langle r^2\rangle_\pi^{\rm exp} \approx (0.672\ {\rm fm})^2$. The pion decay constant is reproduced to be $F_\pi \approx 94$ MeV for both models, while its empirical value is $F_\pi = 93.2$ MeV. All the numerical results are listed in Table 1.

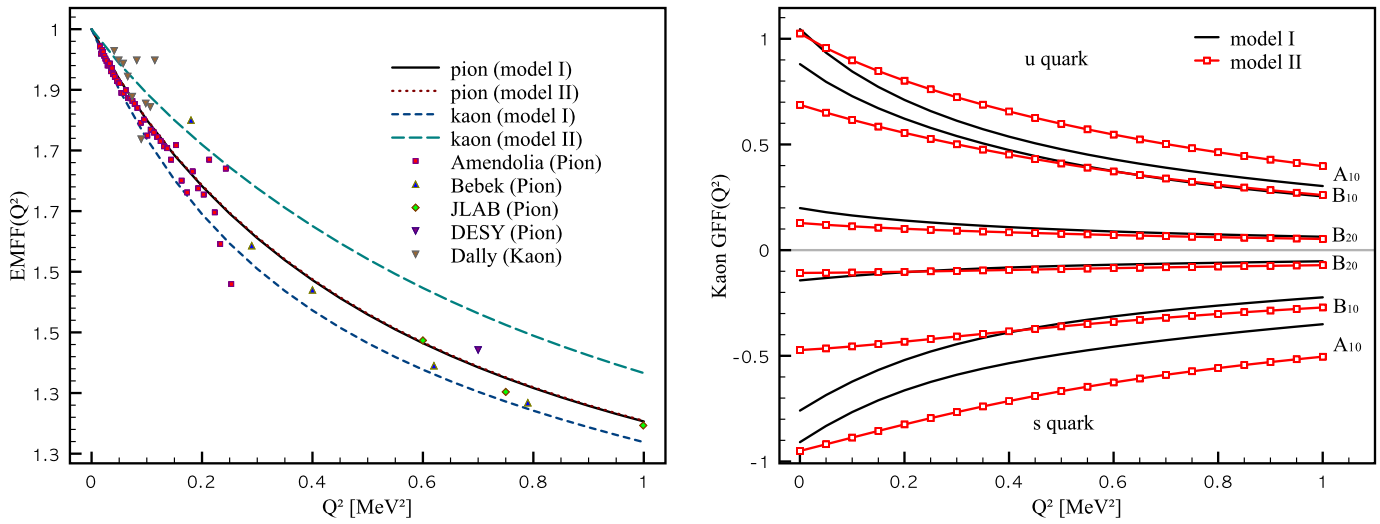

Fig. 1. (Color online.) Electromagnetic form factors of the pion and kaon from model I and model II as functions of Q^2 in the left panel. The experimental data are taken from Refs. [21–24,26,27]. Kaon generalized form factors, $A_{10}^{K,f}$, $B_{10}^{K,f}$, and $B_{20}^{K,f}$, as functions of Q^2 for each flavor, based on model I (solid) and model II (square) in the right panel.

Table 1
The results of the decay constants and charge radii of the pion and kaon from model I and model II, respectively. We have used $m_{u,d} = 5$ MeV, $m_s = 180$ MeV, $1/\bar{R}^4 = (200\ \text{MeV})^4$, and $1/\bar{\rho} = 600$ MeV.

ϕ	Model	M_0	F_ϕ	$F_\phi^{\text{phen.}}$	$\langle r^2\rangle_\phi^{\text{theo.}}$	$\langle r^2\rangle_\phi^{\text{exp.}}$
π	I	350 MeV	94.23 MeV	93.2 MeV	$(0.673\ \text{fm})^2$	$[(0.672 \pm 0.008)\ \text{fm}]^2$
	II	343 MeV	94.43 MeV		$(0.672\ \text{fm})^2$	
K	I	350 MeV	100.17 MeV	113 MeV	$(0.639\ \text{fm})^2$	$[(0.560 \pm 0.031)\ \text{fm}]^2$
	II	407 MeV	118.64 MeV		$(0.560\ \text{fm})^2$	

In contrast, the kaon EM form factors depend on which model we are using. The results of model I are underestimated, being compared with the experimental data [27]: For example, the kaon charge radius turns out to be $\langle r^2\rangle_K^{\text{theo.}} = (0.639\ \text{fm})^2$, which is about 10% larger than the experimental one $\langle r^2\rangle_K^{\text{exp.}} = (0.560\ \text{fm})^2$. In addition, we have the smaller value of the kaon decay constant $F_K = 100.17$ MeV in comparison to the corresponding empirical value $F_K = 113$ MeV. These sizable deviations from the data have been already observed in our previous work [10], and can be understood by the absence of the meson-loop corrections (MLC) which is essential for the cases with the explicit flavor SU(3) symmetry breaking [28]. Hence, to remedy this problem for the kaon case, one may consider the MLC coming from the mesonic fluctuations around the saddle point. However, since it is rather involved, we take a more phenomenological stand on this problem. So, model II can be regarded as a phenomenological way in confronting with the experimental data. We now fit the value of M_0 to reproduce the experimental value for the kaon electric charge radius. The fitted value $M_0 = 407$ MeV brings also about the kaon decay constant $F_K = 118.64$ MeV which is in good agreement with the data. We note that the nonlocal contributions to the electromagnetic form factors of the pion and kaon, which were already discussed in Ref. [10], are about (30–40)%. All the numerical results can be found in Table 1.

Once all the relevant parameters are fixed as discussed above (see Table 1), we can proceed to compute the generalized form factors of the kaon within the two models. As for the pion form factors, one can refer to our previous work [5]. In the left panel of Fig. 1, we depict the results from model I in solid (pion) and shot-dashed (kaon) curves, where as those from model II are drawn in dotted (pion) and long-dashed (kaon) curves. Being different from the pion case, it is necessary to consider the up and strange quarks separately in Eq. (2). However, the up and strange vector form factors of the kaon must satisfy the charge conservation at $Q^2 = 0$ as follows:

$$\frac{2}{3}A_{10}^{K,u}(0) - \frac{1}{3}A_{10}^{K,s}(0) = 1. \tag{17}$$

In the right panel of Fig. 1, we show the results of the up and strange generalized vector and tensor form factors. The results from model I are drawn in solid curves, whereas those from model II are distinguished by putting squares. The six curves in the upper part correspond to the up form factors and those in the lower part illustrate the strange ones. One can observe from the numerical results that the difference between the results from the two different models is noticeable in general apart from the B_{20}. Before we derive the probability densities of the polarized quarks, it is very convenient to parameterize the form factors [1]:

$$A_{10}^{\phi,f}(Q^2) \to \frac{A_{10}^{\phi,f}(0)}{1 + Q^2/M_{A_{10}^{\phi,f}}^2},$$
$$B_{n0}^{\phi,f}(Q^2) \to \frac{B_{n0}^{\phi,f}(0)}{[1 + Q^2/(p_n M_{B_{n0}^{\phi,f}}^2)]^{p_n}}, \tag{18}$$

where the $M_{A_{n0}^{K,f}}$ and $M_{B_{n0}^{K,f}}$ denote the pole masses corresponding to the flavor form factors. Note that we employ a simple monopole and p-pole type parametrizations for the vector and tensor form factors, respectively. Considering the condition $p > 1.5$ for the regular behavior of the probability density at $b_\perp \to 0$ [29] and following Ref. [1], we take $p_1 = p_2 = 1.6$ as a trial. These parametrized form factors are also very useful in analyzing the lattice simulation [1]. Using the numerical results for the generalized form

Table 2
Results for the parametrized form factors in Eq. (18) and $\langle b_y^{K,q}\rangle$ for model I and model II.

Model	Quark	$A_{10}^{K,q}(0)$	$M_{A_{10}^{K,q}}$	$B_{10}^{K,q}(0)$	$M_{B_{10}^{K,q}}$	$B_{20}^{K,q}(0)$	$M_{B_{20}^{K,q}}$	$\langle b_y^{K,q}\rangle$
I	$q=u$	1.045	0.647 GeV	0.880	0.726 GeV	0.199	0.748 GeV	0.168 fm
	$q=s$	−0.909	0.772 GeV	−0.760	0.709 GeV	−0.143	0.806 GeV	0.166 fm
II	$q=u$	1.025	0.894 GeV	0.687	0.898 GeV	0.128	0.918 GeV	0.133 fm
	$q=s$	−0.950	1.081 GeV	−0.473	1.272 GeV	−0.108	1.520 GeV	0.100 fm

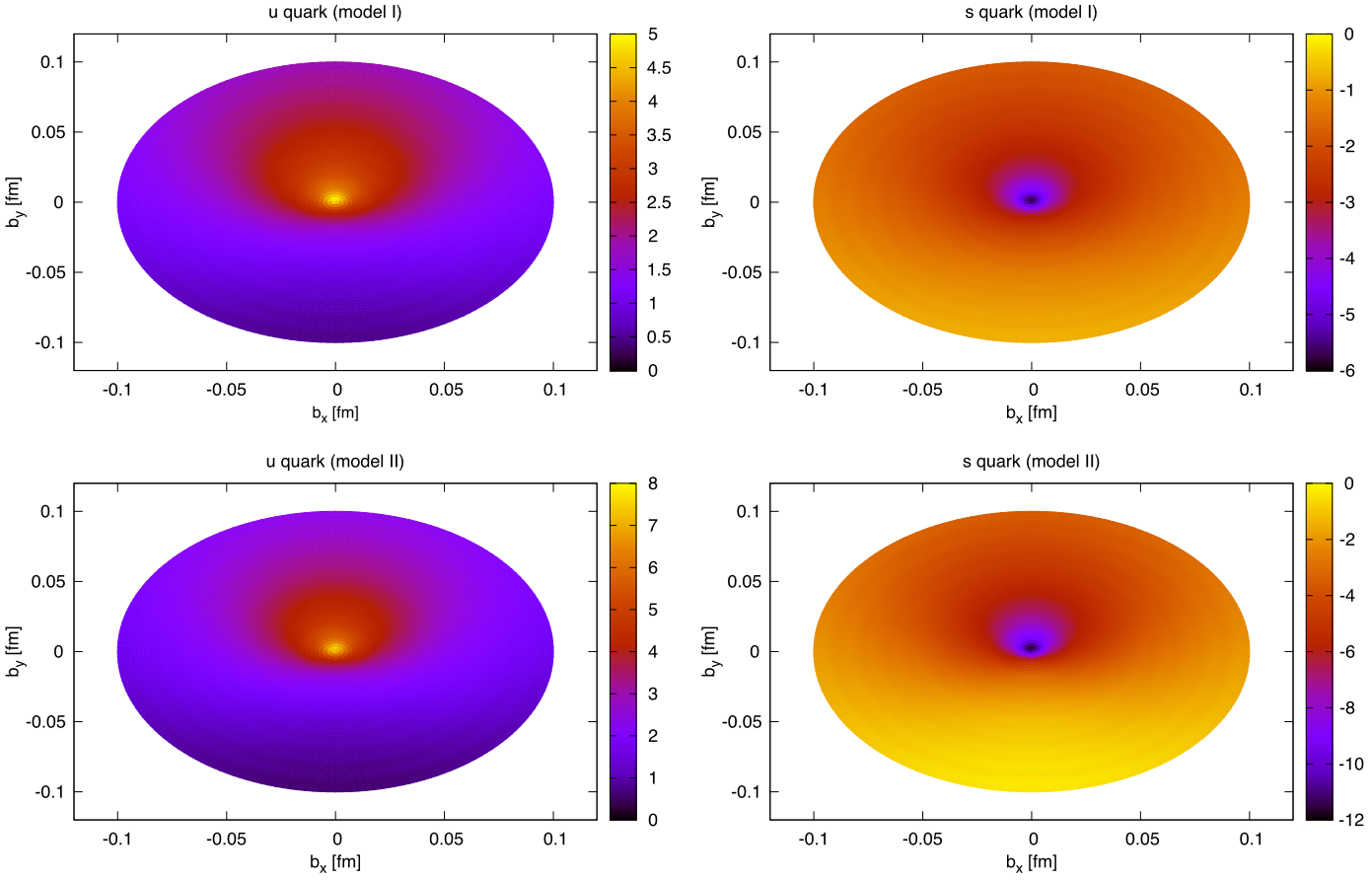

Fig. 2. (Color online.) Polarized quark-spin density $\rho_1^{K,f}$ for the up (left column) and strange (right column) quarks as functions of the impact parameters b_x and b_y for model I (upper panels) and II (lower panels).

factors drawn in the left panel of Fig. 1 and Eq. (18), we extract the numerical values for the parametrized form factors as

$$(M_{A_{10}^{K,u}}, M_{B_{10}^{K,u}}, M_{B_{20}^{K,u}}) = (0.647, 0.726, 0.748)\ \text{GeV},$$
$$(M_{A_{10}^{K,s}}, M_{B_{10}^{K,s}}, M_{B_{20}^{K,s}}) = (0.772, 0.709, 0.806)\ \text{GeV} \qquad (19)$$

for model I and

$$(M_{A_{10}^{K,u}}, M_{B_{10}^{K,u}}, M_{B_{20}^{K,u}}) = (0.894, 0.898, 0.918)\ \text{GeV},$$
$$(M_{A_{10}^{K,s}}, M_{B_{10}^{K,s}}, M_{B_{20}^{K,s}}) = (1.081, 1.272, 1.520)\ \text{GeV} \qquad (20)$$

for model II. The results of the pole masses from model II turn out to be in general larger than those from model I, which indicates that the form factors from model II decrease less slowly than those from model I, as shown in Fig. 1. The pole masses of the pion tensor form factors [5] $M_{B_{10}^{\pi,u}} = 0.761$ GeV and $M_{B_{20}^{\pi,u}} = 0.864$ GeV[1] can be compared with those from the lattice simulation, (0.756 ± 0.095) GeV and (1.130 ± 0.265) GeV, respectively [18]. Note that these lattice data are extrapolated values to $m_\pi = 140$ MeV from the higher pion mass $m_\pi \approx 600$ MeV. In Ref. [34], the Holdom–Terning–Verbeek (HTV) nonlocal-interaction model was employed to compute the tensor form factors for the pion. Their results are qualitatively compatible with ours given in Ref. [5]. All the numerical results are summarized in Table 2 in addition to the values of the generalized form factors at $Q^2 = 0$.

We are now in a position to consider the quark-spin probability density $\rho_n^{\phi,q}$, defined in Eq. (6), using our numerical results for the generalized form factors. For definiteness, we choose $s_\perp = +1$ explicitly in Eq. (7) and take the absolute values for the densities. After performing the Fourier transform of the form factors, we show the numerical results as functions of the two-dimensional impact-space parameters, i.e. b_x and b_y as shown in Fig. 2. As already

[1] We note that there was an error in Ref. [5] related to the tadpole diagram. The contribution from this diagram is essentially zero for the tensor form factors due to its antisymmetric nature. However, correcting the error brings about negligible changes in the numerical results.

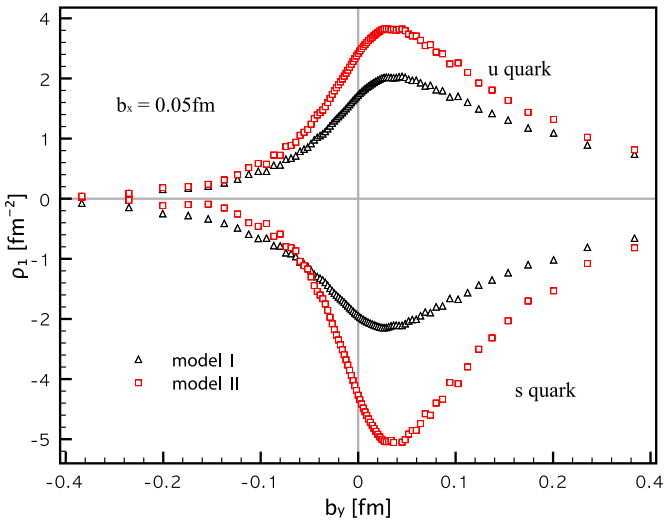

Fig. 3. (Color online.) Profiles of the probability densities at $b_x = 0.05$ fm for the u quark (upper-two curves) and s quark (lower-two curves) for the model I (solid) and II (square).

shown in Ref. [5] and understood from Eq. (7), the unpolarized-quark probability density ($s_\perp = 0$) must be symmetric under the rotation with respect to the z axis, being perpendicular to the b_x–b_y plane. Hence, we do not see any interesting structures from them. On the contrary, when the quark inside the meson is polarized ($s_\perp = +1$), there appears tilted structures signaling the spin structure inside the meson. In Fig. 2, we show the numerical results for the polarized densities from model I (upper-two panels) and from model II (lower-two panels). In the left (right) column, we depict them for the up (strange) quarks. One can clearly observe the distortions of the surfaces due to the polarization. For instance, in Fig. 3, we draw the profiles of probability densities of the polarized up and strange quarks as functions of b_y at $b_x = 0.05$ fm, separately for each model. While the peak positions are very similar to each other, their strengths are different. These structural differences within the densities can be measured via the *average* shift of the peak position along the b_x direction as follows:

$$\langle b_y^{\phi,f}\rangle = \frac{\int d^2b_\perp\, b_y \rho_1^{\phi,f}(b_\perp, s_\perp)}{\int d^2b_\perp\, \rho_1^{\phi,f}(b_\perp, s_\perp)} = \frac{1}{2m_\phi}\frac{B_{10}^{\phi,f}(0)}{A_{10}^{\phi,f}(0)}. \tag{21}$$

Using this, we obtain $\langle b_y^{\phi,u}\rangle = 0.168$ fm and $\langle b_y^{\phi,s}\rangle = 0.166$ fm for model I, and $\langle b_y^{\phi,u}\rangle = 0.133$ fm and $\langle b_y^{\phi,s}\rangle = 0.100$ fm for model II. In the previous work, using Eq. (21), we obtain $\langle b_y^{\pi}\rangle = 0.161$ fm, which is compatible with the lattice calculation $\langle b_y^{\pi}\rangle = (0.151 \pm 0.024)$ fm, being extrapolated to $m_\pi = 140$ MeV [1], which is similar to that of the kaon from model I. However, it turns out that the result for the kaon is about 30% smaller than that for the pion from model II. In other words, if one considers the phenomenologically preferable results, i.e. model II, the difference in the polarized densities for the pion and kaon becomes more obvious, which implies that the polarization effect of the spin inside the pion gets more evident than inside the kaon.

Anticipating the results from lattice QCD in near future, we present the relevant numerical results at $\mu = 2$ GeV which is a usual scale of the lattice simulation. For this purpose, we want to take into account the renormalization-group (RG) evolution [4,30] as follows:

$$B_{n0}(Q^2, \mu) = B_{n0}(Q^2, \mu_0)\left[\frac{\alpha(\mu)}{\alpha(\mu_0)}\right]^{\gamma_n/(2\beta_0)}, \tag{22}$$

where we have used the anomalous dimensions $\gamma_1 = 8/3$ and $\gamma_2 = 8$, and $\beta_0 = 11N_c/3 - 2N_f/3$ ($N_c = 3$ and $N_f = 3$ in the present case). Thus, the powers in the LO evolution equation are given as 4/27 and 4/9, respectively, for $n = 1$ and $n = 2$, which indicate that the dependence of the tensor charge on the normalization point turns out to be rather weak. Note that the anomalous dimension is simply the same as that for the nucleon tensor charge [31]. We also take $\Lambda_{\rm QCD} = 0.248$ GeV which was also used in evolving the nucleon tensor charges and anomalous magnetic moments [32,33]. Since the normalization point of the present model is around 0.6 GeV, whereas the lattice calculation was carried out at $\mu = 2$ GeV, the scale factors turn out to be

$$B_{10}^{\phi,f}(Q^2, \mu = 2\ \text{GeV}) = 0.89 B_{10}^{\phi,f}(Q^2, \mu_0 = 0.6\ \text{GeV}),$$
$$B_{20}^{\phi,f}(Q^2, \mu = 2\ \text{GeV}) = 0.70 B_{20}^{\phi,f}(Q^2, \mu_0 = 0.6\ \text{GeV}). \tag{23}$$

The corresponding results for the tensor charges at $\mu = 2$ GeV are listed in Table 3.

5. In the present work, we aimed at investigating the spin structure of the kaon, based on the nonlocal chiral quark model from the instanton vacuum. We first evaluated the generalized form factors for the kaon, i.e. vector and tensor form factors for the moments $n = 1, 2$. We calculated the flavor vector and tensor form factors of the kaon with explicit flavor SU(3) symmetry breaking considered. In order to improve the electromagnetic form factors of the kaon, which was studied previously [10], we treated the constituent-quark mass at zero virtuality of the quark as a free parameter to fit the experimental data. The vector properties of the pion were almost not changed, whereas those of the kaon were shown to be much improved by using the higher value of the constituent-quark mass. Both the results for the pion and kaon were in good agreement with the data.

Having evaluated the generalized vector and tensor form factors of the kaon, we proceeded to compute the probability densities of the polarized quark inside the kaon. In doing so, we parametrized the form factors, employing the simple monopole and p-pole type parameterizations for the vector and tensor ones. Using the parametrized results, we computed the probability densities of the unpolarized and polarized quarks inside the kaon as functions of the impact parameters, which reveal the spin structures of the kaon. Anticipating the data from the lattice simulation in near future, we also presented the results of the tensor charges, evolving them from the present scale $\mu_0 \approx 600$ MeV to $\mu = 2$ GeV which is a scale often used in the lattice simulations.

We summarize the important observations in the present work:

- The electromagnetic form factor of the pion is reproduced quantitatively well for both models, whereas that of the kaon is well described within model II, i.e. the phenomenological one, compared to the original model (model I) in which there is no free parameter. This difference can be understood by the absence of the $1/N_c$ meson-loop corrections in the present work, which will improve the results of the original model.
- Due to the explicit flavor SU(3) symmetry breaking, the up and strange form factors turn out to be asymmetric with respect to the interchange of up and strange quarks, i.e. V-spin transformation, being different from the pion case. In general we find that the strange form factors are relatively flat in comparison to the up form factors.
- In parametrizing the form factors, we find that model II provides larger pole masses (0.894–1.520) GeV than those from model I (0.647–0.806) GeV. Note that the results of model I are closer to those of the pion.

Table 3
Renormalization-group (RG) evolution of the results for the $B_{10}^{K,q}(0)$ and $B_{20}^{K,q}(0)$ at the scale $\mu = 2$ GeV with $m_K = 495$ MeV for model I and model II. We also write the results for the pion.

Model I			Model II			Pion [5]	
Quark	$B_{10}^{K,f}(0)$	$B_{20}^{K,f}(0)$	Quark	$B_{10}^{K,f}(0)$	$B_{20}^{K,f}(0)$	$B_{10}^{\pi,u}(0)$	$B_{20}^{\pi,u}(0)$
u	0.783	0.139	u	0.611	0.090	0.217	0.034
s	−0.676	−0.100	s	−0.421	−0.076		

- Considering the tensor form factors, we find that the probability density for the polarized quarks get distorted. The degree of this distortion can be measured by the deviation of the average value of $\langle b_y^{K,f} \rangle$ from zero. In model II, the deviation depending on quark species is seen more obviously, i.e. $\langle b_y^{K,(u,s)} \rangle = (0.133, 0.100)$ fm, while almost no difference is observed for model I.
- The RG evolution of the present results brings about the tensor charges as follows: $B_{10}^{K,u} = (0.611\text{–}0.783)$, $|B_{10}^{K,s}| = (0.421\text{–}0.676)$, $B_{20}^{K,u} = (0.090\text{–}0.139)$, and $|B_{20}^{K,s}| = (0.076\text{–}0.100)$ at the renormalization scale $\mu = 2$ GeV, theoretical uncertainties of the present model being taken into account.

As we have shown in the present work, the generalized form factors play a role of revealing the internal spin structures of mesons. While it is very difficult to get access directly to the spin structures of mesons, the lattice data will shed light on understanding them. Moreover, the generalized form factors with different operators and with higher moments will further show us how the quarks inside the kaon behave more in detail. Thus, it will be of great interest to investigate them in the future.

Acknowledgements

The authors are grateful to B.G. Yu and Gh.-S. Yang for fruitful discussions. S.i.N. is thankful to the hospitality of the Hadron Theory Group at Inha University during his visit, where this work was performed. The work of H.Ch.K. was supported by Basic Science Research Program through the National Research Foundation of Korea (NRF) funded by the Ministry of Education, Science and Technology (grant number: 2010-0016265). The work of S.i.N. was supported by the grant NRF-2010-0013279 from National Research Foundation (NRF) of Korea.

References

[1] D. Brommel, et al., QCDSF/UKQCD Collaboration, Phys. Rev. Lett. 101 (2008) 122001.
[2] T. Frederico, E. Pace, B. Pasquini, G. Salme, Phys. Rev. D 80 (2009) 054021.
[3] L. Gamberg, M. Schlegel, Phys. Lett. B 685 (2010) 95.
[4] W. Broniowski, A.E. Dorokhov, E.R. Arriola, Phys. Rev. D 82 (2010) 094001.
[5] S.i. Nam, H.-Ch. Kim, Phys. Lett. B 700 (2011) 305.
[6] D. Diakonov, V.Y. Petrov, Nucl. Phys. B 272 (1986) 457.
[7] M. Musakhanov, Eur. Phys. J. C 9 (1999) 235.
[8] M. Musakhanov, arXiv:hep-ph/0104163.
[9] M. Musakhanov, Nucl. Phys. A 699 (2002) 340.
[10] S.i. Nam, H.-Ch. Kim, Phys. Rev. D 77 (2008) 094014.
[11] E.V. Shuryak, Nucl. Phys. B 203 (1982) 93.
[12] D. Diakonov, V.Y. Petrov, Nucl. Phys. B 245 (1984) 259.
[13] D. Diakonov, Prog. Part. Nucl. Phys. 51 (2003) 173.
[14] T. Schäfer, E.V. Shuryak, Rev. Mod. Phys. 70 (1998) 323.
[15] S.i. Nam, H.-Ch. Kim, Phys. Rev. D 75 (2007) 094011.
[16] M. Diehl, L. Szymanowski, Phys. Lett. B 690 (2010) 149.
[17] G.A. Miller, Phys. Rev. Lett. 99 (2007) 112001.
[18] D. Brommel, et al., QCDSF/UKQCD Collaboration, Eur. Phys. J. C 51 (2007) 335.
[19] S.i. Nam, H.-Ch. Kim, Phys. Lett. B 647 (2007) 145.
[20] D. Diakonov, M.V. Polyakov, C. Weiss, Nucl. Phys. B 461 (1996) 539.
[21] S.R. Amendolia, et al., NA7 Collaboration, Nucl. Phys. B 277 (1986) 168.
[22] S.R. Amendolia, et al., Phys. Lett. B 178 (1986) 435.
[23] C.J. Bebek, et al., Phys. Rev. D 9 (1974) 1229.
[24] J. Volmer, et al., The Jefferson Lab F(pi) Collaboration, Phys. Rev. Lett. 86 (2001) 1713.
[25] V. Tadevosyan, et al., Jefferson Lab F(pi) Collaboration, Phys. Rev. C 75 (2007) 055205.
[26] P. Brauel, et al., Z. Phys. C 3 (1979) 101.
[27] E.B. Dally, et al., Phys. Rev. Lett. 45 (1980) 232.
[28] S.i. Nam, Phys. Rev. D 79 (2009) 014008.
[29] M. Diehl, Ph. Hägler, Eur. Phys. J. C 44 (2005) 87.
[30] V. Barone, A. Drago, P.G. Ratcliffe, Phys. Rept. 359 (2002) 1.
[31] H.-Ch. Kim, M.V. Polyakov, K. Goeke, Phys. Rev. D 53 (1996) 4715.
[32] T. Ledwig, A. Silva, H.-Ch. Kim, Phys. Rev. D 82 (2010) 034022.
[33] T. Ledwig, A. Silva, H.-Ch. Kim, Phys. Rev. D 82 (2010) 054014.
[34] A.E. Dorokhov, W. Broniowski, E. Ruiz Arriola, Phys. Rev. D 84 (2011) 074015.